Protein Density Gradients on Surfaces

Isabelle Caelen, Hui Gao, and Hans Sigrist*

Centre Suisse d'Electronique et de Microtechnique SA (CSEM), rue Jaquet-Droz, 1, CH-2007 Neuchâtel, Switzerland

Received August 20, 2001. In Final Form: November 28, 2001

Gradients of biologically active proteins can be obtained by applying photochemical reactions. A photosensitive polysaccharide-based polymer (OptoDex) is used to covalently immobilize proteins on surfaces. Gradients of proteins are generated by varying the dose of light during the photoimmobilization. Probe proteins conserve their catalytic activity or immunological binding characteristics when linked to surfaces exemplified by silicon nitride or polystyrene. Heterogeneous immunoreactions between photoimmobilized antigens and antibodies showed an optimum binding efficiency at an antigen density of approximatly 1.3 ng/mm^2.

1. Introduction

Microarrays of biomolecules are increasingly used in research and clinical applications to specifically detect, identify, and quantitate target biomolecules that are present in complex biological fluids.[1−5] Microarray technology combines advantages of multiplexing at high feature densities, economy of reagents, fast screening, and—in specific array configurations—averaging of recorded signals over many identical spots on the same surface. Customizing the chip pattern for each kind of experiment is an opportunity to test different parameters, such as the concentration of applied reagents or the nature of the protein.[6]

Gradients of biomolecules represent a powerful tool to investigate interactions in two different ways. First, gradients of different concentrations of immobilized molecules may serve to estimate, in a single step, optimum binding to probing molecules when a solution containing target molecules is applied. With microarrays, such an approach can be carried out in parallel for different molecules. Generation of calibration features in microarrays enables the analysis and quantitation of different analytes. Second, in nature, density gradients of molecules are essential to activate or inhibit biological functions. Gradients of macromolecules on material surfaces may help to investigate and quantify gradient related phenomena.

Covalent immobilization of biomolecules on surfaces is a first and important step in performing heterogeneous bioassays.[7,8] Chemical features applied to immobilize biomolecules will affect the binding efficiency between immobilized probe molecules and solute target molecules: under optimal conditions, probe molecules should conserve their 3D conformation and present accessible binding sites for the interaction with target molecules.[9−12]

Surface density gradients[13] of immobilized proteins on material substrates can be generated by light-sensitive reactions.[14] The approach allows the investigation of protein surface density on the molecular interactions with solute analytes.[15−17] In summary, protein is mixed with a photolinker polymer.[18,19] The mixture is deposited (Figure 1A), dried, and irradiated with light. In the example shown, the photolinker polymer is a polysaccharide-based polymer, multiply substituted with aryldiazirines. Exposure to light generates exceptionally reactive carbenes[20] (Figure 1B). Carbenes react within microseconds with covalent chemical bonds of adjacent surface materials or biomolecules and, thus, generate irreversible links between the biomolecules and the surface.

The radiation energy used for aryldiazirine activation is not destructive for biological functions under the conditions used in this work, and as proteins do not absorb at 350 nm, quenching of the aryldiazirine functions is insignificant. The polysaccharide-based photolinker polymer used in this investigation simulates the native environment of proteins and stabilizes biomolecules by providing numerous valences for hydrogen bonding. Retention of the native structure of the protein is primordial for its subsequent interaction with other molecules.

* To whom correspondence should be addressed: e-mail, hans.sigrist@csem.ch.

(1) Haab, B. B.; Dunham, M. J.; Brown, P. O. http://genomebiology.com/2001/2/2/research/0004/.

(2) Fodor, S. P. A.; Rava, R. P.; Huang, X. C.; Pease, A. C.; Holmes, C. P.; Adams, C. L. *Nature* **1993**, *364*, 555−556.

(3) Joos, T. O.; Schrenk, M.; Höpfl, P.; Kröger, K.; Chowdhury, U.; Stoll, D.; Schörner, D.; Dürr, M.; Herik, K.; Rupp, S.; Sohn, K.; Hämmerle, H. *Electrophoresis 2000* **2000**, *21*, 2641−2650.

(4) Lueking, A.; Horn, M.; Eickhoff, H.; Büssow, K.; Lehrach, H.; Walter, G. *Anal.Biochem.* **1999**, *270*, 103−111.

(5) Walter, G.; Büssow, K.; Cahill, D.; Lueking, A.; Lehrach, H. *Curr. Opin. Microbiol.* **2000**, *3*, 298−302.

(6) Bernard, A.; Michel, B.; Delamarche, E. *Anal. Chem.* **2001**, *73*, 8−12.

(7) Lok, B. K.; Cheng, Y.-L.; Robertson, C. R. *J. Colloid Interface Sci.* **1983**, *91*, 104−116.

(8) Nygren, H.; Werthen, M.; Stendberg, M. *J. Immunol. Methods* **1987**, *101*, 63−71.

(9) Dierks, S.; Butler, J.; Richerson, H. *Mol. Immunol.* **1986**, *23*, 403−411.

(10) Schwab, C.; Bosshard, H. R. *J. Immunol. Methods* **1992**, *147*, 125−134.

(11) Butler, J. E.; Ni, L.; Nessler, R.; Joshi, K. S. *J. Immunol. Methods* **1992**, *150*, 77−90.

(12) Yeung, C.; Purves, T.; Kloss, A. A.; Kuhl, T. L.; Sligar, S.; Leckband, D. *Langmuir* **1999**, *15*, 6829−6836.

(13) Jeon, N. L.; Dertinger, S. K. W.; Chiu, D. T.; Choi, I. S.; Stroock, A. D.; Whitesides, G. M. *Langmuir* **2000**, *16*, 8311−8316.

(14) Hypolite, C. L.; McLernon, T. L.; Adams, D. N.; Chapman, K. E.; Herbert, C. B.; Huang, C. C.; Distefano, M. D.; Hu, W.-S. *Bioconjugate Chem.* **1997**, *8*, 658−663.

(15) Caelen, I.; Bernard, A.; Juncker, D.; Michel, B.; Heinzelmann, H.; Delamarche, E. *Langmuir* **2000**, *16*, 9125−9130.

(16) Duschl, C.; Sévin-Landais, A.-F.; Vogel, H. *Biophys. J.* **1996**, *70*, 1985−1995.

(17) Gee, A. P.; Langone, J. J. *Anal. Biochem.* **1981**, *116*, 524−530.

(18) Barié, N.; Rapp, M.; Sigrist, H.; Ache, H. J. *Biosens. Bioelectron.* **1998**, *13*, 855−860.

(19) Gao, H.; Kislig, E.; Oranth, N.; Sigrist, H. *Biotechnol. Appl. Biochem.* **1994**, *20*, 251−263.

(20) Liu, M. T. H. *Chemistry of diazirines*; Liu, M. T. H., Ed.; CRC Press: Boca Raton, FL, 1992; Chapter 7-9.

10.1021/la0113217 CCC: $22.00
Published on Web 03/01/2002

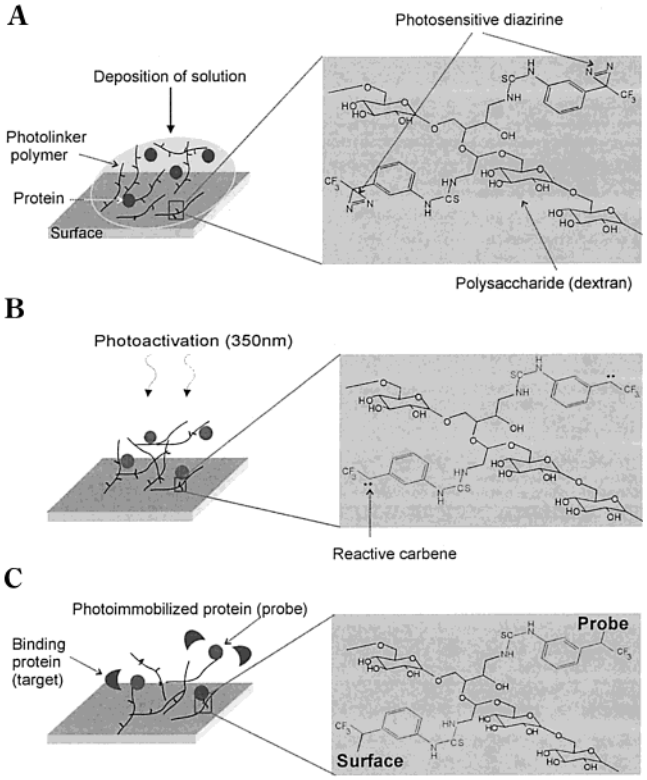

Figure 1. Photolinker polymer mediated protein immobilization. Protein immobilization by light is attained by mixing protein probes with the photolinker polymer OptoDex. The solution is deposited on a selected surface (A). After drying, the sample is irradiated at 350 nm. Photoactivation of the aryldiazirine leads to the formation of reactive carbenes (B). Some carbenes undergo insertion reactions with covalent bonds of probe proteins, others bind to the material surface. After removal of noncovalent attached protein by washing, the surface is probed with target proteins, for example, labeled antibodies (C).

In this study, ink-jet printing and photoimmobilization of biomolecules have been used to generate covalent-bonded protein microarrays on surfaces with different densities of immobilized proteins by varying the dose of light. The efficiency of probe molecule binding to surfaces is quantitated by analyzing the interaction with chromogenic enzyme substrates or fluorescent-labeled target analytes (Figure 1C). The photoimmobilization process combines several advantages:[21,22] (i) The photoreaction is efficient, is fast, and occurs in a single step. (ii) Except for light, no specific reaction conditions are required. (iii) Preactivation of the surface or of the functional groups of the probe biomolecule is not necessary and (iv) simultaneous multicomponent immobilization is possible. (v) If desired, local addressibility can be effected by combining masking techniques or laser writing for example.[23,24]

2. Materials and Methods

2.1. Substrate Materials. Silicon nitride and polystyrene were representative material substrates for metal oxides and organic polymers, respectively. Chip-sized pieces (12 mm × 12 mm) were cut from Si_3N_4-coated wafers and sonicated in isopropanol for 30 min. Ninety six well immunoplates (Nunc immunomodule polysorb, Polylabo, Switzerland) served as polystyrene substrate.

2.2. Proteins and Chemical Reagents. Alkaline phosphatase was obtained from Sigma (Sococchim SA, Switzerland). OptoDex was prepared by thiocarbamoylation of aminodextran with 3-(trifluoromethyl)-3-(*m*-isothiocyanophenyl)diazirine. Mouse-IgG and Cy3-anti-mouse IgG were obtained from Milan (Milan Analytica AG, La Roche, Switzerland). ^{14}C-radiolabeled mouse IgG and anti-mouse IgG were prepared by reductive methylation[25] using ^{14}C-formaldehyde (Amersham Pharmacia Biotech, Switzerland). Cy3-labeled mouse IgG was obtained by reaction of the previous IgG with Cy3-*N*-hydroxysuccinimide ester according to the recommendations of the manufacturer (Cy3 reactive dye pack, Amersham). The number of fluorophores per molecule of IgG was 1.5 for mouse-IgG and 2.3 for anti-mouse IgG. Deionized water or Millipore water (R > 18.2 MΩ cm^{-1}) produced with a Milli-Q purification unit (Millipore) was used in this work. Phosphate buffered saline (PBS) was prepared by mixing 50 mM Na_2HPO_4 (Merk AG, Switzerland), 50 mM NaH_2PO_4 (Merk), and 150 mM NaCl (Fluka Chemie AG, Switzerland) in deionized water. The pH of the solution was adjusted to 7.4. Solutions of Tween 20 (Merk) 0.02% (v/v) in PBS as washing buffer and 1% BSA (bovine serum albumin, Sigma) in PBS as blocking buffer were prepared.

2.3. Surface Immobilization. Twenty four wells of a 96 ELISA immunoplate were filled with a mixture of alkaline phosphatase and Optodex (weight ratio of 1:8). Each well received a final sample volume of 40 μL containing 200 ng of alkaline phosphatase. After the samples were dried for 1 h at 30 mbar vacuum and 2 h at 5 × 10^{-2} mbar, the wells were irradiated for different lengths of time with an Oriel lamp (Oriel 300 W Solar Simulator, Oriel Instruments, L.O.T. Suisse, Switzerland) with an irradiance of 11.2 mW/cm^2 at 365 nm. The washing procedure consisted of incubating each well with 150 μL of the washing buffer (three times 5 min), three times 5 min with 150 μL of PBS, and 3 times with 150 μL of deionized water under permanent shaking of the immunoassay plate.

Immunobinding investigation was carried out by mixing mouse-IgG or labeled mouse-IgG with OptoDex (0.25:0.5 mg/mL of 1% PBS in water). The solution was spotted onto Si_3N_4 chip surfaces with the ink-jet printer (Nano-Plotter, GeSim mbH, Germany). After the printed arrays were dried for 2 h in a vacuum (5 × 10^{-2} mbar), chips were irradiated with the Oriel lamp. The chips were placed in wells (24-well Falcon plates) and washed as detailed above with 1.5 mL of solution for each washing step.

2.4. Enzyme Assay and Immunoassay. Alkaline phosphate substrate solution (100 μL/well) was applied, and the plate was incubated at 37 °C. This defined the starting time for the enzymatic reaction. Enzymatic activity was quantified by registrating hydrolyzed substrate at 405 nm with an ELISA Reader (Spectra Max 340, Molecular Devices).

Before quantitative immunoassays were performed on Si_3N_4 substrates, photobonded antibody microarrays were blocked with the solution of BSA for 30 min at room temperature. Blocking buffer was removed carefully, and Cy3-labeled anti-mouse IgG (20 μg/mL in 1% BSA/PBS) was applied (125 μL/chip). Chips were incubated for 45 min at room temperature, washed 3 times for 5 min with the washing solution, 3 times for 5 min with PBS, and 3 times for 5 min with deionized water (all 1.5 mL/well), and blown dried with N_2.

Immunoreagents and surface densities of on-chip immunoreactions were quantitated by measuring retained radioactivity by scintillation counting or by analyzing surface fluorescence. For radioactive measurements, individual chips were placed in scintillation vials with 5 mL of scintillation fluid (Ultima Gold, Packard Biosciences BV, The Netherlands) and the radioactivity was determined with a Tri-Carb 2300TR β-counter (Packard Instrument Co., USA). Each sample was measured for 2 min. Fluorescent samples were analyzed with the 428 Array Scanner (Affymetrix, USA). Surface densities were determined by applying the Imagene software (Imagene 4, Biodiscovery Inc, USA).

(21) Sigrist, H.; Collioud, A.; Gao, H.; Luginbühl, R.; Sänger, M.; Sundarababu, G. *Opt. Eng.* **1995**, *34*, 2339−2348.
(22) Sänger, M.; Sigrist, H. *Sens. Actuators, A* **1995**, *51*, 83−88.
(23) Herbert, C. B.; McLernon, T. L.; Hypolite, C. L.; Adams, D. N.; Hu, W.-S. *Chem. Biol.* **1997**, *4*, 731−737.
(24) Philipona, C.; Chevolot, Y.; Léonard, D.; Mathieu, H. J.; Sigrist, H.; Marquis-Weible, F. *Bioconjugate Chem.* **2001**, *12*, 332−336.
(25) Jentoft, N.; Dearborn, D. G. *J. Biol. Chem.* **1979**, *254*, 4359−4365.

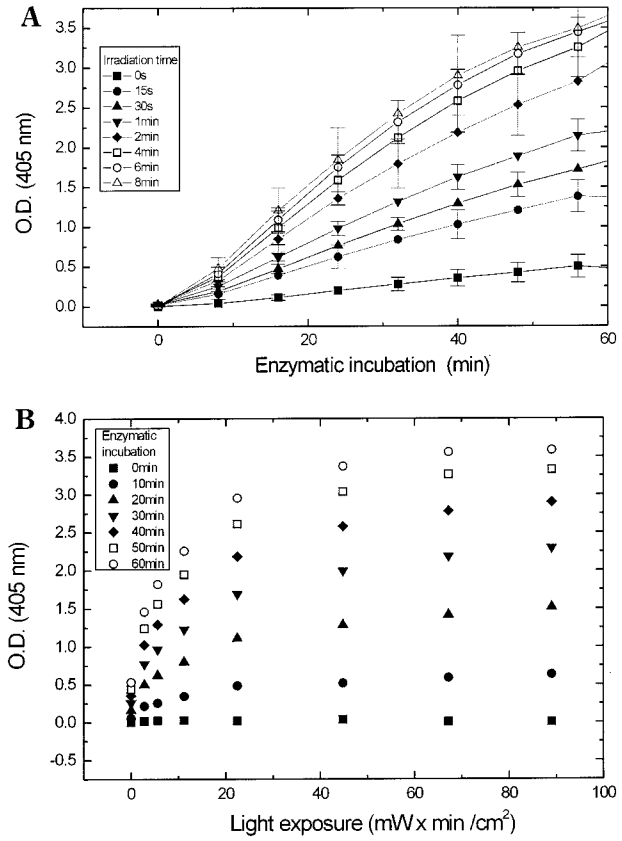

Figure 2. Photoimmobilization of alkaline phosphatase. The enzymatic hydrolysis of *p*-nitrophenyl phosphate to *p*-nitrophenol and phosphate by photoimmobilized alkaline phosphatase is recorded. Triplicate samples of alkaline phosphatase were photoimmobilized for the indicated length of time and product formation rates were monitored by recording *p*-nitrophenol production at 405 mn. (A) Hydrolysis rates increased with increasing irradiation times. (B) Relating the catalytic activity to light exposure (irradiance × irradiation time) revealed nonlinear saturation behavior at each incubation time.

3. Results and Discussion

3.1. Photoimmobilization of Alkaline Phosphatase. The first set of experiments documents the photoimmobilization of alkaline phosphatase on polystyrene. The enzymatic activity of photoimmobilized alkaline phosphatase was registered by following in situ the formation of hydrolytic products from the enzyme substrate (Figure 2). Surface-associated enzymatic activity of photobonded alkaline phosphatase increased with increasing irradiation time (Figure 2A). The initial slopes are a measure of the hydrolytic rate. It thus gives a quantitative measure of the catalytically active enzyme. The curves demonstrate that irradiation time is a key parameter for controlling the amount of enzyme on the surface: for an irradiation from 15 s to 8 min, the rate of the substrate hydrolysis increases by a factor of about 3. Figure 2B reveals the direct dependence of the photoimmobilization reaction on the relative amount of hydrolyzed substrate. Several thermodynamic parameters determine the rate of hydrolysis[26] and limit the substrate/enzyme complex formation. In the first minutes, the diffusion of the substrate to the surface-immobilized enzyme on the wells is essential. This parameter is crucial for short incubation times as illustrated by the initial slopes of the curves in Figure 2B. With extended incubation time however, substrate complexation and hydrolysis depend predominantly on the number of immobilized enzyme molecules and, consequently, on the irradiation intensity used for enzyme photoimmobilization. The profile of the curves reveals that initially the immobilization is fast and saturates at a certain enzyme density.

Background signal intensity is low in the absence of illumination. This indicates that very few proteins persistently physisorb on polystyrene or on Optodex. Since the dextran-based photolinker polymer is present in large excess over probe molecules, the photolinker polymer passivates the surface by "blocking" access to polystyrene. This property is attractive for bioassays, in particular immunoassays, where nonspecific binding of proteins to target surfaces are desirably prevented.[27−30]

3.2. Antigen Immobilization. Results obtained in the previous experiment have shown that different irradiation intensities enabled the formation of surface-density gradients of an immobilized enzyme, while conserving its biological activity. In the approach presented in Figure 3, nanodroplets of a solution of mouse-IgG and Optodex were homogeneously deposited and printed on Si_3N_4 chips in microarray formats (Figure 3A). In the experiment shown in Figure 3, different sample volumes were applied per spot: 1 (a), 2 (b), 3 (c), and 4 nL (d). Deposition of different volumes leads to different spot diameters (from ≈300 μm to ≈500 μm after drying). Chips were exposed to different lengths of irradiation time (I) with the same UV source, rinsed, and dried before analysis. Inserts in Figure 3B show images of array sections of Cy3-labeled mouse IgG photoimmobilized with OptoDex. The quantity of surface-bound IgG, illustrated by the different fluorescence signal intensities registered, depends on the duration of exposure to light. The presence of minor bright zones adjacent to the spots is a rinsing artifact: the wash solution carries away proteins that are not photoimmobilized. These proteins physisorb to nonpassivated Si_3N_4 surrounding the spot (see below). This phenomenon is enhanced for short light exposures: with a low amount of IgG immobilized, higher quantities of protein are washed off and thus available for physisorbtion. This effect can be controlled, for example, by including BSA (1% BSA in PBS) in the first rinsing solution. Such a treatment effects the dilution of IgG. Additionally, BSA competes for IgG physisorption on bare Si_3N_4. For none or low (0.93 mW min/cm^2) illumination, the recovered fluorescence is close to background values, contrasting with the high fluorescence of physisorbed molecules. OptoDex efficiently passivates Si_3N_4 surfaces and eliminates IgG physisorption as expected from observations obtained with alkaline phosphatase on polystyrene.

Quantitative measurement of surface densities was obtained with fluorescent-labeled IgG or radiolabeled IgG. Radioactivity retained on Si_3N_4 chips after photoimmobilization was detected by scintillation counting on exhaustively washed chips. Surface density was determined by relating measured radioactivity to the specific radioactivity of applied ^{14}C-mouse IgG and the surface area occupied. In contrast to the radioactivity measurements, fluorescence detection yielded mere relative signal

(26) Tipton, K. F. *Enzyme Assays—A Practical Approach*; Eisenthal, R., Danson, M. J., Eds.; Oxford University Press: New York, 1992; Chapter 11.

(27) Prime, K. L.; Whitesides, G. M. *J. Am. Chem. Soc.* **1993**, *115*, 10714−10721.

(28) Roberts, C.; Chen, C. S.; Mrksich, M.; Martichonok, V.; Ingber, D. E.; Whitesides, G. M. *J. Am. Chem. Soc.* **1998**, *120*, 6548−6555.

(29) Szleifer, I. *Biophys. J.* **1997**, *72*, 595−612.

(30) Yang, Z.; Galloway, J. A.; Yu, H. *Langmuir*. **1999**, *15*, 8405−8411.

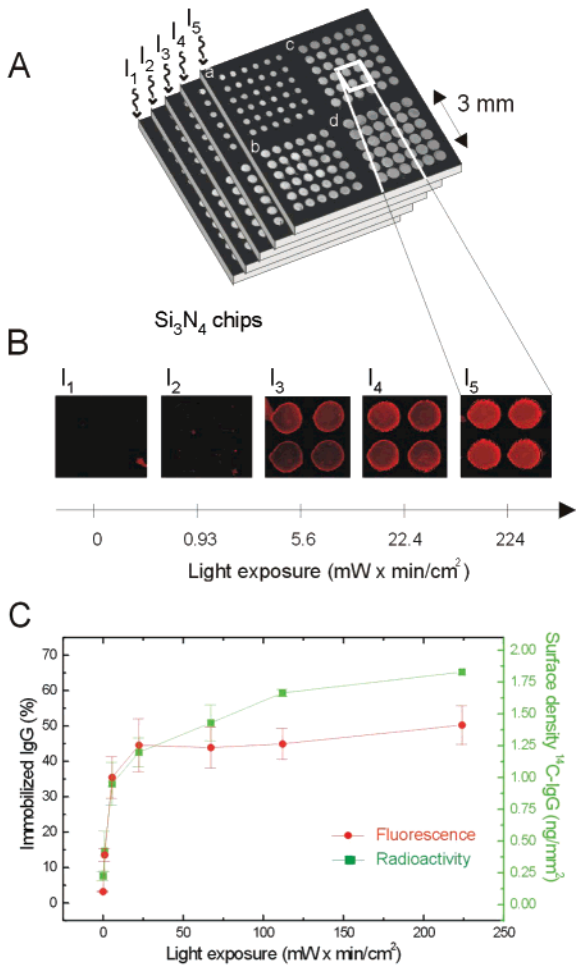

Figure 3. Photoimmobilization of antigens on Si_3N_4. Radiolabeled or fluorescence-labeled mouse-IgG was deposited on Si_3N_4 and exposed to different light exposures (A). Part B depicts fluorescence microscopy images of selected parts of protein arrays consisting of piezo-tip printed Cy3-labeled mouse IgG. Both radioactive and fluorescent tracing of the antibodies indicated nonlinear saturating binding kinetics (C).

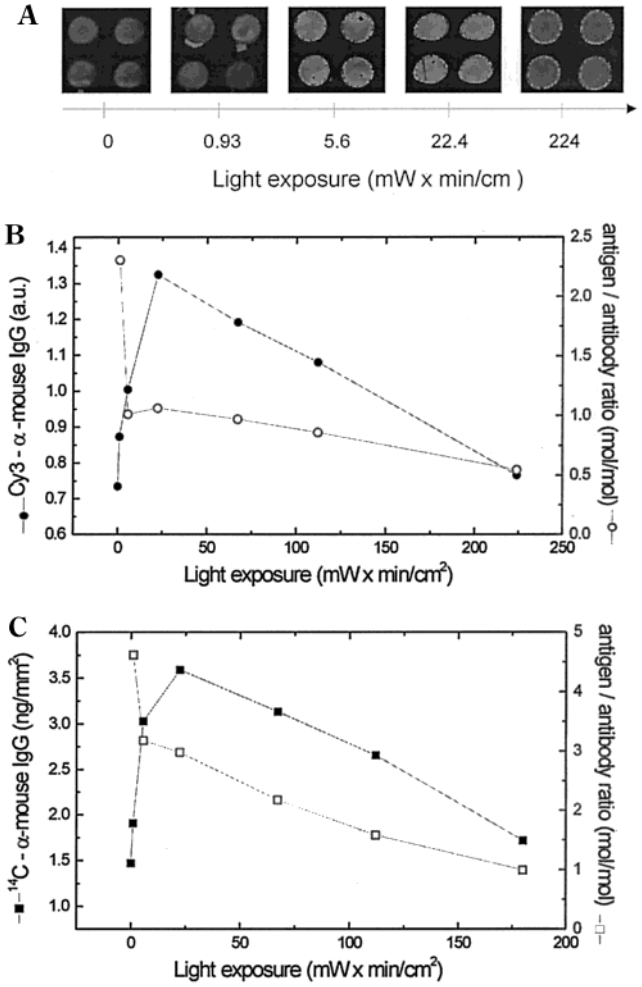

Figure 4. Immunocomplexation of photobonded antigens. (A) Fluorescence microscopy of Si_3N_4 chip sections with surface-immobilized antigens (mouse IgG) after immunocomplexation with Cy3-labeled antibodies (Cy3-anti mouse IgG). It is observed by fluorescence (B) and radioactivity (C) tracing that antibody binding decreases with increasing antigen surface density. Both detection systems confirm optimal antibody binding for light exposure of 22.4 mW min/cm^2.

intensities. The detected fluorescence was correlated with the radioactivity measurements assuming that the initial amount of fluorescent-labeled IgG deposited was identical to the initial amount of radioactive-labeled IgG (about 3 ng/mm^2). Radioactivity and fluorescence measurements plotted as a function of the light exposure time (Figure 3C) showed similar surface densities: the signals increase quickly at low light exposure and saturate at a surface density of protein below 2 ng/mm^2. The differences at extended exposure times of relative amount of immobilized IgG between the fluorescence and radioactivity measurements are explained by fluorescence quenching. High fluorophore concentrations lower the signal intensity.[31]

3.3. Immunocomplexation of Arrayed Antigens. Antigen microarrays, as shown in Figure 3, are useful to study the binding of antibodies to photoimmobilized antigens as a function of antigen surface density. Figure 4A illustrates such an experiment: immunocomplexation was carried out by exposing arrays of nonlabeled-mouse IgG (antigens) on Si_3N_4 to a solution of Cy3-labeled anti-mouse IgG (antibodies). Detection of immunocomplexed antibodies revealed that their presence on the surface matches the pattern of the mouse antigens previously immobilized. The immunointeraction demonstrated different binding characteristics than the light-dependent antigen immobilization showed in Figure 3B. Importantly, the immunorecognition layer shows a relatively high fluorescence "background" in the first image of Figure 4A, revealing that binding of antibodies occurs. Several factors can contribute to residual antibody sorption at low overall OptoDex surface occupation: First, few antigens can be present on the surface and antibodies could efficiently immunoreact. Second, if no illumination occurs, molecules of OptoDex are adsorbed on the surface and can be washed away during the rinsing step. Consequently, when the solution of antibodies is applied, surface adsorption of the antibody can occur. Third, noncovalent interactions between physisorbed OptoDex and antibodies may favor weak binding of antibodies to the linker polymer. The washing conditions used (Tween 0.02%, PBS, and water) are probably not sufficient at low surface densities to displace the weak interactions between IgG and OptoDex or between IgG and the surface.

The surface density of immunocomplexed antibodies was quantitated using radioactivity and fluorescence measurements. The surface densities based on fluorescence measurements (Figure 4B) were calibrated using

(31) Hassan, M.; Landon, J.; Smith, D. S. *FEBS Lett.* **1979**, *103*, 339−341.

experimental data as obtained with Cy3-labeled mouse IgG in Figure 3. The known specific radioactivity of ^{14}C-α-mouse IgG allowed calculation of the molecular surface density (Figure 4C). A same behavior is observed for both curves: the extent of antibodies binding increases fast at low-light doses, reaches a maximum, and decreases as the surface density of antigens further increases. Photodestruction of immobilized antigens with increasing exposure time could be one possible explanation. However, results obtained in the enzyme binding study, show increased enzymatic activity up to 90 mW min/cm^2. This illustrates that photodestruction of alkaline phosphatase does not occur under photobonding conditions used. Moreover, ligand binding competition is known to occur at high antigen density as observed in heterogeneous ELISA assays. The range of protein binding to Si_3N_4 at saturation is not identical for the two types of measurements, however. Radioactivity measurements exhibit a broader range (from ≈1.5 to 3.5 ng/mm^2) and yield higher values than fluorescence ones. Several reasons can explain this difference: First, the sensitivity of the radioactivity detection is higher than that of fluorescence detection. Net radioactivity is measured in the picogram range, whereas fluorescence reports on surface densities in the nanogram range. Second, fluorescence quenching is most probable at increased surface densities; this further limits the sensitivity at elevated surface densites. Third, the scintillation counter gives a measure of radioactivity based on the entire chip whereas the fluorescent measurements are averaged only within the spots. This could contribuate to higher values for radioactivity when compared to fluorescence measurements. Last, fluorescence and radiolabel are not identical in chemical terms and, in addition, the extent of label substitution is different. The last factor can effect a distinct bioreactivity of either of the two labeled antibodies and could have consequences on the efficiency of immunocomplexation.

The values shown in plots B and C of figure 4 report on antibody binding efficiency: the ratio between the quantity of immunocomplexed antibodies and the photobonded antigens measured in function of light exposure. The first measuring point, corresponding to the background signal of both antigen and antibody, is not relevant and was not considered in the graphic presentation. Measured by radioactivity or fluorescence, the curves show a similar behavior. Proportionally fewer antibodies are bound with increasing antigen density on the surface. Several causes can affect the recognition of an antigen by its antibody from solution. Access to the immobilized antigen and the steric hindrance[32−34] between molecules may significantly influence the extent of immunocomplexation. With increased illumination time, more photons can be adsorbed by the photolinker polymer to form chemical bonds. The network of cross-linked dextran progressively densifies, forming a "gel"-like 3D scaffold covalently bonded to the surface. This could have several consequences on the efficiency on the binding between antigens and antibodies: First, antibody access becomes diffusion controlled as the dextran network gets denser. Second, the lack of space between dextran molecules may prevent antibodies from acquiring binding conformation and thus limit the complexation between the two partners. Third, in a confined space, an antibody bound to an antigen could block other antibodies from binding to the same antigen or could prevent these antibodies from penetrating the dextran network.

For optimized immunoassays, high complexation efficiency is required with a minimum quantity of immobilized antigens. Under the experimental conditions applied in this work, an exposure of 22.4 mW min /cm^2 yields an optimal complexation with antibodies for an antigen density of 1.3 ng/mm^2.

Conclusion

Protein-based microarrays are emerging tools in protein−protein interaction studies. The approach combines the advantages to generate high-density arrays, to economize precious reactants, to increase the self-consistency of the results by averaging over multiple identical spots, and to customize bioprinted zones by including reference and quality markers. Even though technical aspects in making arrays or analyzing the data generated are progressing, on-chip bioreactions are limited by the intrinsic nature of biomolecules that interact. The presented approach uses a polysaccharide-based polymer, OptoDex, that prevents denaturation of proteins and acts both as a linker of biomolecules and as a blocking reagent preventing nonspecific binding. The high degree of substitution of OptoDex with photoactivatable groups (about 9 mol of aryldiazirine per mole of photolinker polymer) enables irreversible immobilization of the biomolecules. The surface density attained depends on the dose of light used for photoimmobilization. This work details the influence of the density of surface immobilized antigens on antibody binding efficiency and denotes the importance to optimize the relative quantity of surface-bound molecules in bioassays.

Acknowledgment. We acknowledge E. Delamarche (IBM, Rüschlikon) for carefully reading the manuscript. We are grateful to H. R. Bosshard (University of Zürich) for his continuous support and interest in the work.

LA0113217

(32) Wimalasena, R. L.; Wilson, G. S. *J. Chromatogr.* **1991**, *572*, 85−102.

(33) Fowel, S. L.; Chase, H. A. *J. Biotechnol.* **1986**, *4*, 1−13.

(34) Butler, J.; Spradling, J.; Dierks, S.; Heyermann, H.; Peterman, J.; Suter, M. *Mol. Immunol.* **1986**, *23*, 971−982.